mathematics

MDPI

Article

Topological Properties and Entropy Calculations of Aluminophosphates

Jeyaraj Sahaya Vijay [1], Santiago Roy [1,*], Bheeter Charles Beromeo [1], Mohamad Nazri Husin [2,*], Tony Augustine [1], R.U. Gobithaasan [2] and Michael Easuraja [3]

[1] School of Advanced Sciences, Vellore Institute of Technology, Vellore 632 014, India; sahayavijay.j@vit.ac.in (J.S.V.); charlesbheeter@vit.ac.in (B.C.B.); tony.augustine@vit.ac.in (T.A.)
[2] Special Interest Group on Modelling and Data Analytics (SIGMDA), Faculty of Ocean Engineering Technology and Informatics, Universiti Malaysia Terengganu, Kuala Nerus 21030, Terengganu, Malaysia; gr@umt.edu.my
[3] Department of Chemistry, Arul Anandar College, Karumathur 625 514, India; easuraja@aactni.edu.in
* Correspondence: roy.santiago@vit.ac.in (S.R.); nazri.husin@umt.edu.my (M.N.H.)

Abstract: Topological indices are invariant numerical quantities of a graph that give facts about the structure of graphs and are found to be very helpful in predicting the physical properties of aluminophosphates. The characteristics of aluminophosphates are similar to the characteristics of zeolites. Two examples of current applications are natural gas dehydration and humidity sensors. Researchers in chemistry and materials science are synthesizing new frameworks. There are many layers and holes in these substances. The technique used to predict natural behaviors among the physicochemical characteristics of chemical molecules in their basic network is known as topological indices. This study explains the vertex version of distance-based topological indices, the entropy of topological indices and their numerical analysis.

Keywords: aluminophosphates; vertex-based molecular descriptors; cut method; Shannon's method; correlation coefficient

MSC: 05C09; 05C92; 92E10

Citation: Vijay, J.S.; Roy, S.; Beromeo, B.C.; Husin, M.N.; Augustine, T.; Gobithaasan, R.U.; Easuraja, M. Topological Properties and Entropy Calculations of Aluminophosphates. *Mathematics* **2023**, *11*, 2443. https://doi.org/10.3390/math11112443

Academic Editor: Hilal Ahmad

Received: 21 April 2023
Revised: 17 May 2023
Accepted: 18 May 2023
Published: 25 May 2023

1. Introduction

Aluminophosphate is an essential crystalline microporous material. Due to its well-defined pore structures and high porosities, it has high permeability and selectivity [1,2]. It is available at low prices and provides synthesis and accessibility for various applications. Especially in catalyst preparation, it is used to improve catalyst efficiency and, in process development, to recognize the reaction mechanism [3]. To introduce a particular characteristic, appropriate metals in the periodic table can incorporate aluminophosphates due to their outstanding pore attributes and hydrophilic nature [4]. Accordingly, among solid catalysts, silico aluminophosphate has a worldwide market of billions of USD per annum [5,6]. Moreover, because of water adsorption properties, potential aluminophosphates are available with a superior pore volume greater than 14% in contrast to zeolite frameworks. Therefore, studying their core structure in a thorough conceptual banner is becoming essential to increase aluminophosphates' porosity, efficiency and stability for enhanced applications.

Such aluminophosphate materials can be structurally represented using molecular graphs, in which the vertices stand for atoms and the edges stand for chemical bonds. To extract topological information from such graphs, one can utilize theoretical graph quantifiers, which in turn give valuable functions that have perfect linear relationships with various properties of such materials through graph invariants or, more commonly, structure descriptors.

Quantitative structure–activity relationships (QSAR) and quantitative structure–property relationships (QSPR) can be supported by topological indices, which are among the structural descriptors that provide numerical functions of the structure of a molecule. The derived variables can be used to calculate the chemical and biological properties of the materials. The complex systems of such materials that are difficult to define due to their complexity can be viewed as an objective numerical variable that characterizes them. The numerical variable that describes the networks of these structural applications is called the topological index of a molecular structure. One of the most significant and efficient structural descriptors in the field of advanced materials is the fact that the mathematical functions that can be generated using various graph theoretical approaches can be used to predict the properties of these materials. They are often an addition to quantum chemistry calculations that need a good deal of computing [7–22]. A wide range of indices can be used in research to understand the relationships between structure and properties.

It should be mentioned that very little progress has been made in the inclusion of topological descriptors that are based purely on the connectivity to chemistry-specific characteristics, such as various indicators [23–35], especially for very heavy atoms in such materials for which relativistic impacts are essential.

In a well-known 1948 study [36], the author first introduced the idea of entropy, declaring that the entropy of a probability distribution is known as a measure of unpredictability. Entropy was used to assess the structural details of graphs and chemical networks. Rachhevsky et al. introduced in 1955 the idea of graph entropy based on categorizing vertex orbits [37]. In many disciplines, there has been an increase in the use of graph entropy. Information theory was used in biology and chemistry after initial linguistics and electrical engineering applications. Spontaneous communication is one of the essential innovations [38–43]. Network structural information content was calculated using Shannon's entropy formula [36] in light of this realization. This technique was used to examine living systems using graphs. Graphs are used to investigate biological and chemical networks [44].

This paper studies a set of weighted topological descriptors for chemical molecules. We also investigated how the perfect linear relationship in $QSPR$ and $QSAR$ models can be improved by assigning optimal weights to the vertices of the structure to obtain a realistic topology. Models that include structural instabilities and other quantum chemistry-derived features that control the overall structural stability of chemical substances have also been explored.

2. Computational Theoretical Technique

A graph $G = (V(G), E(G))$, where $V(G)$ is the set of all the vertices of G and $E(G)$ is the set of all the edges of G. The cardinality of $V(G)$ and $E(G)$ is denoted by $|V(G)| = M$ and $|E(G)| = N$, respectively. The number of edges incident to u is represented by the degree of a vertex u. It is denoted as $d_G(u)$. The length of the shortest uv-path is called the distance $d_G(u, v)$ between two vertices $u, v \in V(G)$. We used $d(v)$ and $d(u, v)$ for $d_G(v)$ and $d_G(u, v)$, respectively, in this study.

To count the vertices and evaluate which quantity is closest to the end vertices of $e = uv$, we must first recall the two numbers based on vertices and edge distance functions.

- $n_u(e) = |t \in V(G) : d(u, t) < d(v, t)|$
- $n_v(e) = |t \in V(G) : d(v, t) < d(u, t)|$

Further, we list the distance-based and bond additive topological indices in Table 1 derived from the below-mentioned quantitative metrics, such as distance and closeness.

Table 1. Vertex version of distance-based molecular descriptors.

Molecular Descriptors	Mathematical Formula
Wiener Index [16]	$WI_v(G) = \sum_{\{u,v\}\subseteq V(G)} d(u,v)$
Vertex–Szeged Index [9]	$Sz_v(G) = \sum_{e=uv\in E(G)} n_u(e)n_v(e)$
Vertex–Padmakar–Ivan Index [11]	$PI_v(G) = \sum_{e=uv\in E(G)} n_u(e) + n_v(e)$
Vertex–Mostar Index [45]	$Mo_v(G) = \sum_{e=uv\in E(G)} \lvert n_u(e) - n_v(e)\rvert$

With Matlab programming, the provided distance-based and bond additive topological indices could be successfully calculated based on the Djoković–Winkler relationship by finding the equivalence classes of graph structures. For any two edges $e_1 = ab \in E(G)$ and $e_2 = cd \in E(G)$, if $d_G(a,c) + d_G(b,d) \neq d_G(a,d) + d_G(b,c)$ then $e_1\Theta e_2$ is called a Djković–Winkler relation Θ [46,47]; these play a key role in our analytical computation. The graph G that may be isometrically embedded into a hypercube is called a partial cube. Bipartite graphs with transitive Djoković–Winkler relation Θ or cut method [48] can be used to describe partial cubes [47]. Let Θ^*-class be the transitive closure of the Djoković–Winkler relation Θ.

The relation Θ is also transitive and hence an equivalence relation if molecular graph G is a partial cube [49]. Let K be a partial cube with its Θ-classes $\mathcal{F}(K) = \{F_1, F_2, ..., F_r\}$. Let $TI \in \{WI_v, WI_e, W_{ve}, Sz_v, Sz_e, Sz_{ve}, PI_v, S, Gut, Mo, Mo_e, Mo_t, w^+Mo, w^+Mo_e, w^+Mo_t, w^*Mo, w^*Mo_e.w^*Mo_t\}$, Then $TI(K) = \sum_{i=1}^{k}(TI(K/F_i))$ [49].

In this article, we use the following methods to compute distance-based molecular descriptors (see Table 1): [8,49,50]

1. $WI_v(G/F_i) = n_1(F_i)n_2(F_i)$
2. $Sz_v(G/F_i) = |F_i|(n_1(F_i)n_2(F_i))$
3. $PI_v(G/F_i) = |F_i|(n_1(F_i) + n_2(F_i))$
4. $Mo_v(G/F_i) = |F_i||n_1(F_i) - n_2(F_i)|$

3. Results and Discussion

This study discusses aluminophosphate-based molecular sieve structures and their perfect linear relationships with molecular descriptors. The high selectivity, more significant adsorption velocity, higher strength and increased anti-pollution ability produced by the shape and structural optimization increase the consumption effects of the molecular sieve.

Being the first extra-large-pore crystalline material ever made, the extra-large VPI-5, $AIPO$ molecular sieve with 18-ring channels was discovered. The chain-building units used to build VPI-5 and $AIPO$-H_2 contain octahedral Al atoms (coordinated with four framework oxygens and two water molecules). The modest number of extra-large-pore microporous materials with 16-ring channels is very noteworthy. The synthesis of ITQ-51, a previously unreported extra-large-pore silico aluminophosphate ($SAPO$) with 16 ring openings, using the bulky aromatic proton sponge $DMAN$ as an $OSDA$, is presented by Martinez-Franco et al. [51].

The pore openings of aluminophosphate-based molecular sieve structures $T12MR$ (see Figure 1a), $T16MR$ (see Figure 1b) and VPI-5 (see Figure 1c) [51] seem like n mesh. The layer is placed in an n,l,k-dimensional mesh known as a molecular sieve hexagonal mesh $mSHL(n,l,k)$. This layer can be easily stretched to several layers, as shown in Figure 2, and is denoted G, where G is considered a molecular sieve hexagonal mesh $mSHL(n,l,k)$ in this study.

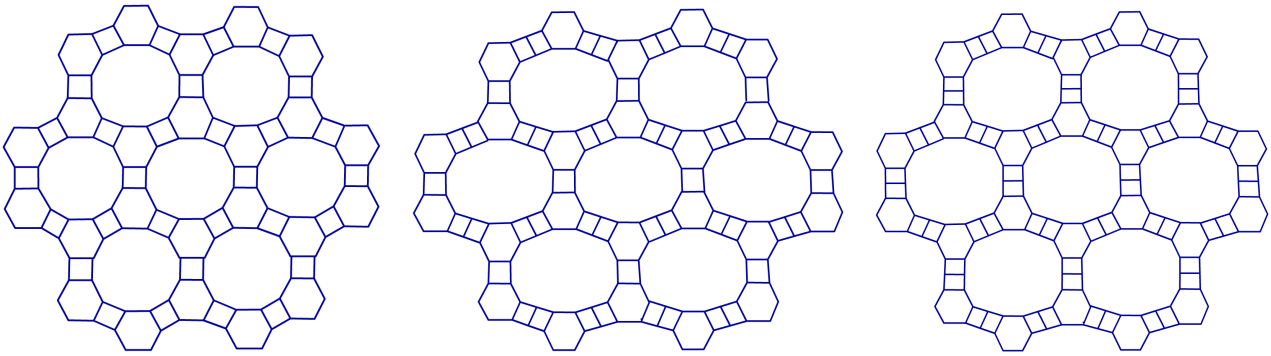

(**a**) *T12MR* (**b**) *T16MR* (**c**) *VPI*-5

Figure 1. Aluminophosphate-based molecular sieve structures.

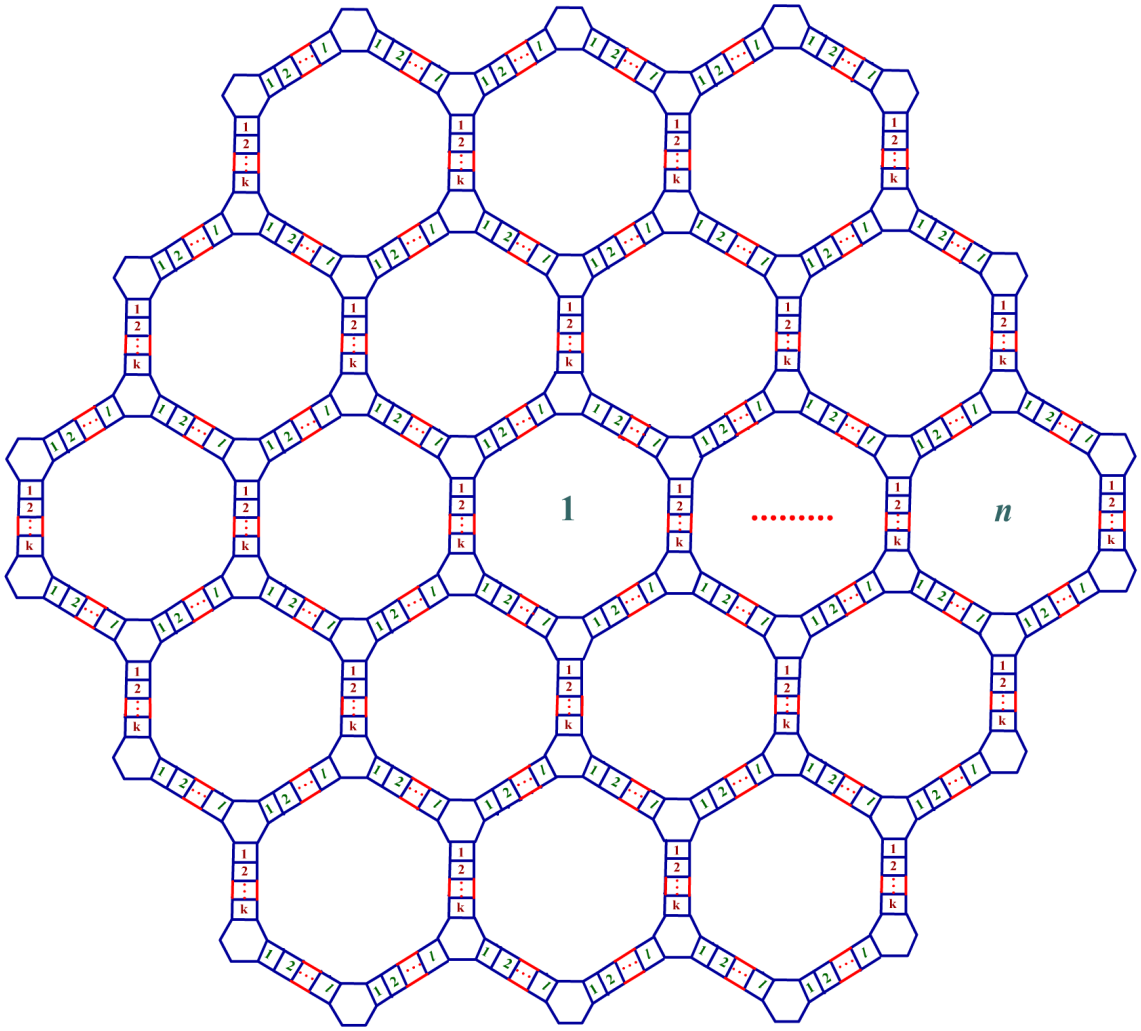

Figure 2. Aluminophosphate-based molecular sieve structure growth $mSHL(n,l,k)$.

3.1. Vertex Distance-Based Topological Indices

In this section, we present an analytical computation of some vertex versions of distance-based topological descriptors for molecular sieve hexagonal mesh $mSHL(n,l,k)$. We used Matlab version 2019 software for analytical computation and also used Flash 8 to construct molecular structure in this study.

Theorem 1. *Let G be a molecular sieve hexagonal mesh $mSHL(n,l,k)$. Then*

$W_v(G) = \frac{2n}{45}(246k^3n^4 - 270k^3n^3 + 100k^3n^2 - 15k^3n - k^3 + 1476k^2ln^4 - 1230k^2ln^3 + 240k^2ln^2 + 60k^2ln - 6k^2l + 2754k^2n^4 - 1260k^2n^3 - 90k^2n^2 + 90k^2n - 9k^2 + 2952kl^2n^4 - 2265kl^2n^3 + 150kl^2n^2 + 285kl^2n - 42kl^2 + 11016kln^4 - 3870kln^3 - 1620kln^2 + 450kln + 144kl + 9882kn^4 + 1845kn^3 - 1630kn^2 - 345kn + 88k + 1968l^3n^4 - 1770l^3n^3 + 440l^3n^2 + 30l^3n - 8l^3 + 11,016l^2n^4 - 4455l^2n^3 - 990l^2n^2 + 405l^2n + 54l^2 + 19764ln^4 + 3690ln^3 - 3260ln^2 - 690ln + 176l + 11502n^4 + 9585n^3 + 1800n^2 - 270n - 72)$

$Sz_v(G) = \frac{n}{60(-1)^k}(174(-1)^k k - 195(-1)^{kn}n - 45(-1)^{3n}(-1)^k + 348(-1)^k l + 2070(-1)^k n - 810(-1)^{kn}n^2 - 1215(-1)^{kn}n^3 + 402(-1)^k - 30(-1)^k k^2 + 10(-1)^k k^3 - 204(-1)^k l^2 - 76(-1)^k l^3 - 45(-1)^k(-1)^n + 9120(-1)^k n^2 + 29,700(-1)^k n^3 + 81648(-1)^k n^4 + 87480(-1)^k n^5 - 288(-1)^k kl + 360(-1)^k kn + 100(-1)^k ln - 45(-1)^{3n}(-1)^k k^2 + 15(-1)^{3n}(-1)^k k^3 - 90(-1)^{3n}(-1)^k l^2 + 30(-1)^{3n}(-1)^k l^3 + 270(-1)^{3n}(-1)^k n^2 + 2025(-1)^{3n}(-1)^k n^3 + 195(-1)^{kn}(-1)^k n + 810(-1)^{kn}kn^2 - 45(-1)^{kn}k^2 n + 405(-1)^{kn}kn^3 - 45(-1)^{kn}k^3 n - 60(-1)^{kn}l^2 n - 1620(-1)^{kn}ln^3 - 240(-1)^k kl^2 - 96(-1)^k k^2 l + 45(-1)^k(-1)^n k - 2760(-1)^k kn^2 + 120(-1)^k k^2 n - 5870(-1)^k kn^3 + 120(-1)^k k^3 n + 22476(-1)^k kn^4 + 10(-1)^k k^4 n + 87480(-1)^k kn^5 + 90(-1)^k(-1)^n l - 7520(-1)^k ln^2 + 3240(-1)^k l^2 n - 10120(-1)^k ln^3 + 120(-1)^k l^3 n + 54672(-1)^k ln^4 + 174960(-1)^k ln^5 - 180(-1)^k(-1)^n n + 810(-1)^{kn}(-1)^k n^2 + 1215(-1)^{kn}(-1)^k n^3 + 90(-1)^{kn}k^2 n^2 + 675(-1)^{kn}k^2 n^3 - 90(-1)^{kn}k^3 n^2 + 135(-1)^{kn}k^3 n^3 + 360(-1)^{kn}l^2 n^2 - 540(-1)^{kn}l^2 n^3 + 45(-1)^{3n}(-1)^k k - 45(-1)^k(-1)^n k^2 - 440(-1)^k k^2 n^2 + 15(-1)^k(-1)^n k^3 + 950(-1)^k k^2 n^3 - 520(-1)^k k^3 n^2 - 8060(-1)^k k^2 n^4 - 10(-1)^k k^3 n^3 + 160(-1)^k k^4 n^2 + 29160(-1)^k k^2 n^5 - 540(-1)^k k^3 n^4 - 630(-1)^k k^4 n^3 + 3240(-1)^k k^3 n^5 + 540(-1)^k k^4 n^4 + 90(-1)^{3n}(-1)^k l - 90(-1)^k(-1)^n l^2 + 440(-1)^k l^2 n^2 + 30(-1)^k(-1)^n l^3 - 8940(-1)^k l^2 n^3 + 200(-1)^k l^3 n^2 - 36896(-1)^k l^2 n^4 + 7380(-1)^k l^3 n^3 + 116640(-1)^k l^2 n^5 - 24704(-1)^k l^3 n^4 + 25920(-1)^k l^3 n^5 - 180(-1)^{3n}(-1)^k n + 270(-1)^k(-1)^n n^2 + 2025(-1)^k(-1)^n n^3 + 285(-1)^{kn}kn + 180(-1)^{kn}ln + 80(-1)^k kl^2 n^2 - 1480(-1)^k k^2 ln^2 - 120(-1)^k k^2 l^2 n + 11720(-1)^k kl^2 n^3 + 4700(-1)^k k^2 ln^3 + 960(-1)^k k^3 ln^2 - 38000(-1)^k kl^2 n^4 - 13904(-1)^k k^2 ln^4 - 2520(-1)^k k^3 ln^3 + 38880(-1)^k kl^2 n^5 + 19440(-1)^k k^2 ln^5 + 2160(-1)^k k^3 ln^4 - 180(-1)^{3n}(-1)^k kn - 1170(-1)^k(-1)^n kn^2 + 30(-1)^k(-1)^n k^2 n + 675(-1)^k(-1)^n kn^3 - 60(-1)^k(-1)^n k^3 n - 360(-1)^{3n}(-1)^k ln - 2340(-1)^k(-1)^n ln^2 + 570(-1)^k(-1)^n l^2 n + 1350(-1)^k(-1)^n ln^3 - 330(-1)^k(-1)^n l^3 n - 240(-1)^{kn}kln - 90(-1)^{kn}(-1)^k k^2 n^2 - 675(-1)^{kn}(-1)^k k^2 n^3 + 90(-1)^{kn}(-1)^k k^3 n^2 - 135(-1)^{kn}(-1)^k k^3 n^3 - 360(-1)^{kn}(-1)^k l^2 n^2 + 540(-1)^{kn}(-1)^k l^2 n^3 + 3680(-1)^k kln + 960(-1)^k k^2 l^2 n^2 - 2520(-1)^k k^2 l^2 n^3 + 2160(-1)^k k^2 l^2 n^4 - 1170(-1)^{3n}(-1)^k kn^2 + 30(-1)^{3n}(-1)^k k^2 n + 675(-1)^{3n}(-1)^k kn^3 - 60(-1)^{3n}(-1)^k k^3 n - 150(-1)^k(-1)^n k^2 n^2 - 225(-1)^k(-1)^n k^2 n^3 + 90(-1)^k(-1)^n k^3 n^2 - 75(-1)^k(-1)^n k^3 n^3 - 2340(-1)^{3n}(-1)^k ln^2 + 570(-1)^{3n}(-1)^k l^2 n + 1350(-1)^{3n}(-1)^k ln^3 - 330(-1)^{3n}(-1)^k l^3 n - 240(-1)^k(-1)^n l^2 n^2 - 900(-1)^k(-1)^n l^2 n^3 + 960(-1)^k(-1)^n l^3 n^2 - 600(-1)^k(-1)^n l^3 n^3 - 285(-1)^{kn}(-1)^k kn - 180(-1)^{kn}(-1)^k ln + 360(-1)^{kn}kln^2 + 60(-1)^{kn}kl^2 n + 60(-1)^{kn}k^2 ln + 1080(-1)^{kn}kln^3 + 800(-1)^k kln^2 + 520(-1)^k kl^2 n + 700(-1)^k k^2 ln - 8720(-1)^k kln^3 - 120(-1)^k k^3 ln - 41552(-1)^k kln^4 + 116640(-1)^k kln^5 - 180(-1)^k(-1)^n kn - 360(-1)^k(-1)^n ln - 150(-1)^{3n}(-1)^k k^2 n^2 - 225(-1)^{3n}(-1)^k k^2 n^3 + 90(-1)^{3n}(-1)^k k^3 n^2 - 75(-1)^{3n}(-1)^k k^3 n^3 - 240(-1)^{3n}(-1)^k l^2 n^2 - 900(-1)^{3n}(-1)^k l^2 n^3 + 960(-1)^{3n}(-1)^k l^3 n^2 - 600(-1)^{3n}(-1)^k l^3 n^3 - 810(-1)^{kn}(-1)^k kn^2 + 45(-1)^{kn}(-1)^k k^2 n - 405(-1)^{kn}(-1)^k kn^3 + 45(-1)^{kn}(-1)^k k^3 n + 60(-1)^{kn}(-1)^k l^2 n - 360(-1)^{kn}kl^2 n^2 + 1620(-1)^{kn}(-1)^k ln^3 - 360(-1)^{kn}k^2 ln^2 + 540(-1)^{kn}kl^2 n^3 + 540(-1)^{kn}k^2 ln^3 + 240(-1)^{kn}(-1)^k kln + 1020(-1)^k(-1)^n kln + 1680(-1)^{3n}(-1)^k kl^2 n^2 + 780(-1)^{3n}(-1)^k k^2 ln^2 - 900(-1)^{3n}(-1)^k kl^2 n^3 - 450(-1)^{3n}(-1)^k k^2 ln^3 - 360(-1)^{kn}(-1)^k kln^2 - 60(-1)^{kn}(-1)^k kl^2 n - 60(-1)^{kn}(-1)^k k^2 ln - 1080(-1)^{kn}(-1)^k kln^3 + 1020(-1)^{3n}(-1)^k kln + 120(-1)^k(-1)^n kln^2 - 300(-1)^k(-1)^n kl^2 n - 210(-1)^k(-1)^n k^2 ln - 900(-1)^k(-1)^n kln^3 + 360(-1)^{kn}(-1)^k kl^2 n^2 + 360(-1)^{kn}(-1)^k k^2 ln^2 - 540(-1)^{kn}(-1)^k kl^2 n^3 - 540(-1)^{kn}(-1)^k k^2 ln^3 + 120(-1)^{3n}(-1)^k kln^2 - 300(-1)^{3n}(-1)^k kl^2 n - 210(-1)^{3n}(-1)^k k^2 ln - 900(-1)^{3n}(-1)^k kln^3 +$

$1680(-1)^k(-1)^n kl^2n^2 + 780(-1)^k(-1)^n k^2ln^2 - 900(-1)^k(-1)^n kl^2n^3 - 450(-1)^k(-1)^n k^2ln^3)$

$$PI_v(G) = \frac{n}{2(-1)^k}(9n - 2l - k + 3kn + 6ln + 3)(3(-1)^{3n}(-1)^k + (-1)^{kn}k - 4(-1)^k l + 12(-1)^k n - (-1)^{kn} + (-1)^{kn}(-1)^k + 6(-1)^k - 2(-1)^k k^2 + 3(-1)^k(-1)^n + 108(-1)^k n^2 - 16(-1)^k kn - 24(-1)^k ln - (-1)^{kn}(-1)^k k - (-1)^k(-1)^n k + 36(-1)^k kn^2 + 4(-1)^k k^2 n - 2(-1)^k(-1)^n l + 72(-1)^k ln^2 - (-1)^{3n}(-1)^k k - 2(-1)^{3n}(-1)^k l)$$

$$Mo_v(G) = \frac{1}{2}(2k^2n - 4kn - 8ln - k^2 - 2l^2 - 2(-1)^n k - 80kn^2 - 72kn^3 + 324kn^4 - 4(-1)^n l - 160ln^2 + 12l^2 n - 144ln^3 + 648ln^4 + 24(-1)^n n + 3(-1)^n + 12n^2 + 84n^3 + 486n^4 + 2k + (-1)^n k^2 - 32k^2n^2 - 4k^2n^3 + 54k^2n^4 + 4l - 8(-1)^l n^2 + 2(-1)^n l^2 + 16(-1)^l n^3 - 84l^2n^2 - 88l^2n^3 + 216l^2n^4 - 36n + 36(-1)^n n^2 - 40kln^2 - 160kln^3 + 216kln^4 - 4(-1)^n kn - 8(-1)^n ln - 4(-1)^n l^2 n + 16kln - 16(-1)^l k^2n^2 + 32(-1)^l k^2n^3 + 2k^2 n - 4(-1)^n k^2n^2 + 8l^2 n - 16(-1)^n l^2n^2 - 8(-1)^n kln + 8kln - 16(-1)^n kln^2) - 3).$$

Proof. Let G be a molecular sieve hexagonal mesh $mSHL(n,l,k)$. Here the total number of vertices of G is denoted $M = 6n - 2kn - 4ln + 6kn^2 + 12ln^2 + 18n^2$ and the total number of edges of G is denoted $N = n^2(9k + 27) - l(-18n^2 + 6n) - n(3k - 3)$. The graph G that may be isometrically embedded into a hypercube is called a partial cube. Bipartite graphs with transitive Djoković–Winkler relation Θ or cut method can be used to describe partial cubes. Let Θ^*-class be the transitive closure of the Djoković–Winkler relation Θ.

Throughout this paper, we discussed two types of Θ^*-classes F_{mi} and F^*_{mi} on G, where $1 \leq m \leq 3$ are depicted in Figure 3. We show different directions of Θ^*-classes $Dd(Th)$ on $mSHL(2,1,1)$ in Figure 4. By applying $Dd(Th)$ on G, G is converted to quotient graphs Q, which is a complete bipartite graph K_2 (see Figure 5). Let $a_j b_j \in K_2$ and let $h(i)$ denotes the number of cut edges in G. To complete the analytical computation by using all mentioned Θ^*-classes (see Figure 4), we now divide the Θ^*-classes of G into two cases.

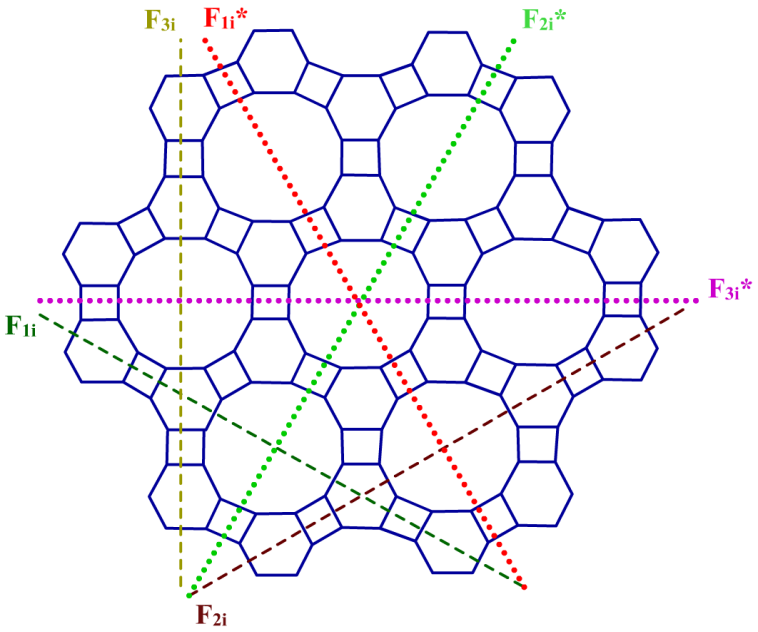

Figure 3. Two types of Θ^*-class F_{fi} and F^*_{fi}.

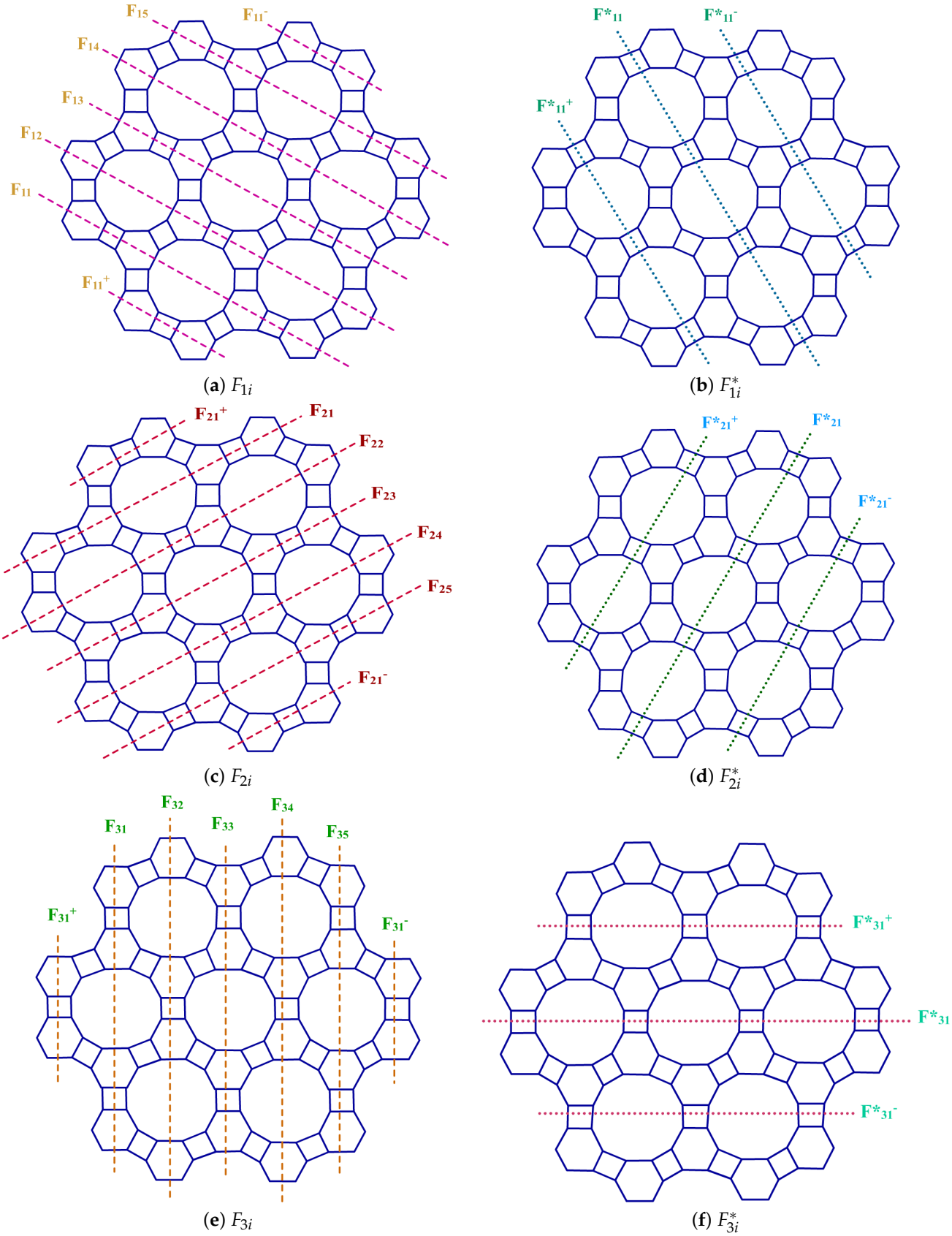

(**a**) F_{1i} (**b**) F^*_{1i}

(**c**) F_{2i} (**d**) F^*_{2i}

(**e**) F_{3i} (**f**) F^*_{3i}

Figure 4. Different directions of Θ^*-classes.

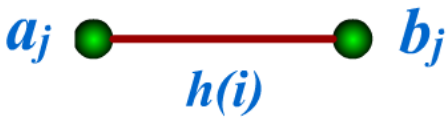

Figure 5. Quotient graph Q.

Case (i): F_{mi} on G; $\{F_{mi}|1 \le m \le 3\}$, $\{F_{mi}|1 \le i \le n-1\}$, $\{F_{mi}|n \le i \le 3n\}$.

For $1 \le j \le 4$, $1 \le i \le 4$, the vertex-weighted a_j, b_j and the strength-weighted $h(i)$ values on vertices of Q are defined below:

$a_1 = (k+2l+3)i^2 + (2-l-k)i$

$a_2 = i(n(2k+6)+l(4n-1)+1) - n(k-1) - 2ln^2 - n^2(k+3)$

$a_3 = (k+2l+3)i^2 + (2-2l)i$

$a_4 = i(4ln - k + n(2k+6)+1) - l(2n^2+2n) + n(k+1) - n^2(k+3)$

$b_j = M - a_j$, where $1 \le j \le 4$.

$h(1) = li + 3i \qquad h(2) = \frac{((-1)^i+1)}{2}(3n - l + ln + 1) - \frac{((-1)^i-1)}{2}(3n + ln)$

$h(3) = ki + 3i \qquad h(4) = \frac{((-1)^i+1)}{2}(3n - k + kn + 1) - \frac{((-1)^i-1)}{2}(3n + kn)$

Case (ii): F^*_{mi} on G; $\{F^*_{mi}|1 \le m \le 3\}$, $\{F^*_{mi}|1 \le j \le n-1, (j-1)l+1 \le i \le jl\}$, $\{F^*_{mi}|nl-l+1 \le i \le nl\}$, $\{F^*_{mi}|1 \le j \le n-1, (j-1)k+1 \le i \le jk\}$ and $\{F^*_{mi}|nk-k+1 \le i \le nk\}$

For $5 \le j \le 8$, $5 \le i \le 6$, the vertex-weighted a_j, b_j and strength-weighted $h(i)$ values on vertices of Q are defined below:

$a_5 = l(2j^2 - 2j + n(4j-2)) - (2j+2n)(l(j-1) - i + 1) + n(j(2k+6)+2) - j(k-3) + j^2(k+3)$

$a_6 = n^2(3k+9) - l(-6n^2+4n) - n(k-5) + n(4i+4l-4ln-4)$

$a_7 = n(j(4l+6)+2) - (2j+2n)(k(j-1) - i + 1) + j^2(2l+3) + k(j^2 - j + n(2j-2)) - j(2l-3)$

$a_8 = n^2(6l+9) - k(-3n^2+3n) + n(4i+4k-4kn-4) - n(2l-5)$

$b_j = M - a_j$ where $5 \le j \le 8$

$h(5) = 2n + 2j \qquad h(6) = 4n$

By symmetry, we have $F_{mi^+} = F_{mi^-}$ and $F^*_{mi^+} = F^*_{mi^-}$, and $1 \le m \le 3$ (see Figure 4). Define,

$$(X(G), \circ) = 2\sum_{i=1}^{n-1} 2h(1)(a_1 \circ b_1) + h(3)(a_3 \circ b_3) + \sum_{i=n}^{3n} 2h(2)(a_2 \circ b_2) + h(4)(a_4 \circ b_4) + 2\left[2\sum_{j=1}^{n-1}\sum_{i=(j-1)l+1}^{jl} h(5)(a_5 \circ b_5) + \sum_{i=ln-l+1}^{ln} h(6)(a_6 \circ b_6)\right] + 2\sum_{j=1}^{n-1}\sum_{i=(j-1)k+1}^{jk} h(5)(a_7 \circ b_7) + \sum_{i=kn-k+1}^{kn} h(6)(a_8 \circ b_8),$$

where $(X, \circ) = (W_v, \times), (Sz_v, \times), (PI_v, +)$ and when $(X, \circ) = (W_v, \times)$, $h(i) = 1$, for $1 \le i \le 6$.

$$Y(G) = 2\sum_{i=1}^{n-1} 2h(1)(b_1 - a_1) + h(3)(b_3 - a_3) + \sum_{i=n}^{2n-1} 2h(2)(b_2 - a_2) + h(4)(b_4 - a_4) + 2\left[2\sum_{j=1}^{n-1}\sum_{i=(j-1)l+1}^{jl} h(5)(b_5 - a_5) + \sum_{i=\frac{1}{2}(n-l+ln+1)}^{\frac{1}{2}(n)(l+1)} h(6)(b_6 - a_6) + \sum_{i=\frac{1}{2}(ln-l+2)}^{\frac{ln}{2}} h(6)(b_6 - a_6)\right] + 2\sum_{j=1}^{n-1}\sum_{i=(j-1)k+1}^{jk} h(5)(b_7 - a_7) + \sum_{i=\frac{1}{2}(n-k+kn+1)}^{\frac{1}{2}(n)(k+1)} h(6)(b_8 - a_8) + \sum_{i=\frac{1}{2}(kn-k+2)}^{\frac{kn}{2}} h(6)(b_8 - a_8).$$

Further, an analytical computation of $(X(G), \circ)$ and $Y(G)$ yields the results of Theorem 1.

□

3.2. Vertex Degree-Based Topological Indices

In this section, we implement degree-based molecular descriptors of G. Let G be broken into three different edge sets using the methodology of edge set partition (ESP) of molecular descriptors. For clarity, the ESPs of $mSHL(2,1,1)$ are shown in Figure 6.

The ESPs of G are $|esp(2,2)| = 6n, |esp(2,3)| = 12n, |esp(3,3)| = ((18n^2 - 6n)l + (9k + 27)n^2 - (3k + 15)n)$.

The degree-based molecular descriptors [52–59] presented in Table 2 will help chemists to find the closure values of physiochemical properties by using statistical correlation.

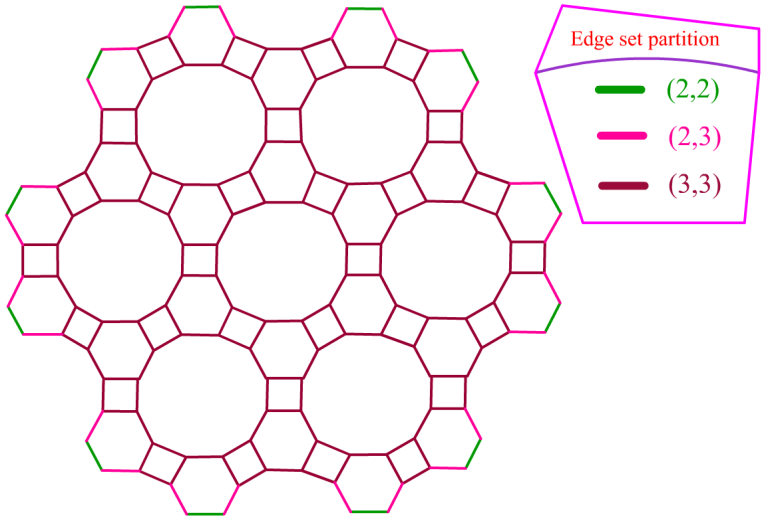

Figure 6. Edge set partitions (ESPs).

Table 2. Different types of vertex versions of degree-based molecular descriptors.

Molecular Descriptors	Mathematical Formula
First Zagreb Index	$M_1(G) = \sum_{uv \in E(G)} [d_u + d_v]$
Second Zagreb Index	$M_2(G) = \sum_{uv \in E(G)} [d_u \times d_v]$
Reduced Second Zagreb Index	$RM_2(G) = \sum_{uv \in E(G)} [(d_u - 1)(d_v - 1)]$
Hyper Zagreb Index	$HM(G) = \sum_{uv \in E(G)} [d_u + d_v]^2$
Augmented Zagreb Index	$AZ(G) = \sum_{uv \in E(G)} [\frac{d_u \times d_v}{d_u + d_v - 2}]^3$
Randić Index	$R(G) = \sum_{uv \in E(G)} [\frac{1}{\sqrt{d_u d_v}}]$
Reciprocal Randić Index	$RR(G) = \sum_{uv \in E(G)} [\sqrt{d_u d_v}]$
Reduced Reciprocal Randić Index	$RRR(G) = \sum_{uv \in E(G)} [\sqrt{(d_u - 1)(d_v - 1)}]$
Harmonic Index	$H(G) = \sum_{uv \in E(G)} [\frac{2}{d_u + d_v}]$
Sum Connectivity Index	$SC(G) = \sum_{uv \in E(G)} \frac{1}{\sqrt{d_u + d_v}}$

We obtain the expressions of degree-based molecular descriptors from Table 2 using the above edge set partitions.

Theorem 2. *Let G be a molecular sieve hexagonal mesh $mSHL(n,l,k)$. Then*

$M_1(G) = 6n(27n - 6l - 3k + 9kn + 18ln - -1)$
$M_2(G) = 3n(81n - 18l - 9k + 27kn + 54ln - -13)$
$RM_2(G) = 6n(18n - 4l - 2k + 6kn + 12ln - -5)$
$HM(G) = 36n(27n - 6l - 3k + 9kn + 18ln - -4)$
$AZ(G) = \frac{9n}{64}(2187n - 486l - 243k + 729kn + 1458ln - 191)$
$R(G) = n(9n - 2l - k + 3kn + 6ln + 26^{\frac{1}{2}} - 2)$
$RR(G) = 3n(27n - 6l - 3k + 9kn + 18ln + 46^{\frac{1}{2}} - 11)$
$RRR(G) = 6n - 2l(-18n^2 + 6n) + 12(2^{\frac{1}{2}})n + 2n^2(9k + 27) - 2n(3k + 15)$
$H(G) = \frac{n}{3}(18n - 4l - 2k + 6kn + 12ln + 11)$
$SC(G) = n(9n - 2l - k + 3kn + 6ln + 26^{\frac{1}{2}} - 2)$.

3.3. Degree-Based Entropy

In this section, we present the numerical analysis and the entropy stability of the given molecular descriptors in Table 2. Further, the section provides instructions on calculating entropy values according to Shannon's method by constructing a probability function from degree-based topological indices. We used Shannon's model to calculate probabilistic entropy because it is the most widely used method [55,59–62]. Using that topological index, the entropy K is calculated as follows:

$$E_k(G) = log(K(G)) - \frac{1}{K(G)}\left(\sum_{uv \in E(G)} (f(e)log(f(e)))\right)$$

By using $M_1(G)$ to calculate the entropy value for G, the calculation procedure is illustrated.

First Zagreb entropy for $mSHL(n,l,k)$

$$\begin{aligned}
&EM_1(G) = \log(6n(27n - 6l - 3k + 9kn + 18ln - 1))\\
&-\frac{(6n)(2+2)\log(2+2) + (12n)(2+3)\log(2+3)}{6n(27n - 6l - 3k + 9kn + 18ln - 1)}\\
&+\frac{((18n^2 - 6n)l + (9k + 27)n^2 - (3k + 15)n)(3+3)\log(3+3)}{6n(27n - 6l - 3k + 9kn + 18ln - 1)}\\
&= \log(6n(9kn + 18ln - 3k - 6l + 27n - 1)) - \frac{48n\log(2) + 60n\log(5)}{6n(9kn + 18ln - 3k - 6l + 27n - 1)}\\
&+\frac{6((18n^2 - 6n)l + (9k + 27)n^2 - (3k + 15)n)\log(6)}{6n(9kn + 18ln - 3k - 6l + 27n - 1)}
\end{aligned}$$

After simplifying this, we obtain

$$\begin{aligned}
EM_1(G) = &\frac{((9k + 18l + 27)n - 3k - 6l - 1)\log(9((k + 2l + 3)n - \frac{k}{3} - \frac{2l}{3} - \frac{1}{9})n)}{(9k + 18l + 27)n - 3k - 6l - 1}\\
&+\frac{6\log(2) + 14\log(3) - 10\log(5)}{(9k + 18l + 27)n - 3k - 6l - 1}
\end{aligned}$$

However, concerning each topological index, its method and 3D plot of entropy (see Figure 7), as mentioned above, can generate any degree-based entropy expressions.

3.4. Numerical Results

The numerical values of distance- and degree-based molecular descriptors utilizing entropy measures generated for G are given in Tables 3 and 4 with the values of the variables n, l and k ranging from 1 to 10.

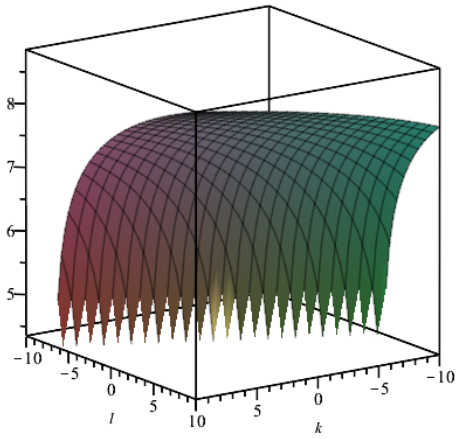

Figure 7. Three-dimensional plot of EM_1.

Table 3. Numerical values for distance-based molecular descriptors.

(*n*, *l* , *k*)	**(1, 1, 1)**	**(2, 2, 2)**	**(3, 3, 3)**	**(4, 4, 4)**	**(5, 5, 5)**
$WI_v(G)$	3024	270,000	4,668,072	37,920,768	198,934,944
$Sz_v(G)$	12,096	2,180,550	59,575,584	665,112,240	4,487,610,096
$PI_v(G)$	1728	59,976	560,592	2,819,448	10,144,560
$Mo_v(G)$	576	27,684	265,776	1,385,064	4,916,352
(*n*, *l* , *k*)	**(6, 6, 6)**	**(7, 7, 7)**	**(8, 8, 8)**	**(9, 9, 9)**	**(10, 10, 10)**
$WI_v(G)$	784,272,816	2,527,739,928	7,013,962,368	17,335,729,008	39,076,777,008
$Sz_v(G)$	21,585,912,126	82,522,470,576	264,389,591,088	743,053,567,968	1,873,931,558,022
$PI_v(G)$	28,958,688	71,033,760	154,482,768	308,200,032	571,213,080
$Mo_v(G)$	14,290,380	34,549,680	76,122,576	149,955,648	280,858,740

Table 4. Numerical values for degree-based molecular descriptors.

(*n*, *l* , *k*)	**(1, 1, 1)**	**(2, 2, 2)**	**(3, 3, 3)**	**(4, 4, 4)**	**(5, 5, 5)**
$M_1(G)$	264	1716	5328	12,072	22,920
$M_2(G)$	366	2514	7902	17,988	34,230
$RM_2(G)$	150	1092	3474	7944	15,150
$HM(G)$	1476	10,080	31,644	72,000	136,980
$AZ(G)$	485.71875	3226.78125	10,068.46875	22,856.0625	43,434.84375
$R(G)$	17.899	101.798	305.6969	683.5959	1290
$RR(G)$	131.3939	856.7878	2662	6034	11,457
$RRR(G)$	82.9706	561.9411	1761	4004	7615
$H(G)$	13.66666667	71.33333333	209	462.6666667	868.3333333
$SC(G)$	17.899	101.798	305.6969	683.5959	1290
(*n*, *l* , *k*)	**(6, 6, 6)**	**(7, 7, 7)**	**(8, 8, 8)**	**(9, 9, 9)**	**(10, 10, 10)**
$M_1(G)$	38,844	60,816	89,808	126,792	172,740
$M_2(G)$	58,086	91,014	134,472	189,918	258,810
$RM_2(G)$	25,740	40,362	59,664	84,294	114,900
$HM(G)$	232,416	364,140	537,984	759,780	1,035,360
$AZ(G)$	73,650.09375	115,347.0938	170,371.125	240,567.4688	327,781.4063
$R(G)$	2177	3401	5015	7073	9629
$RR(G)$	19,418	30,404	44,899	63,391	86,364
$RRR(G)$	12,918	20,237	29,896	42,219	57,530
$H(G)$	1462	2279.666667	3357.333333	4731	6436.666667
$SC(G)$	2177	3401	5015	7073	9629

These values were plotted using the Origin 2020b for a graphical comparison (see Figures 8–10) of the computed topological descriptors below. The three-dimensional plots proved a comparison to the behavior of degree-based indices of G.

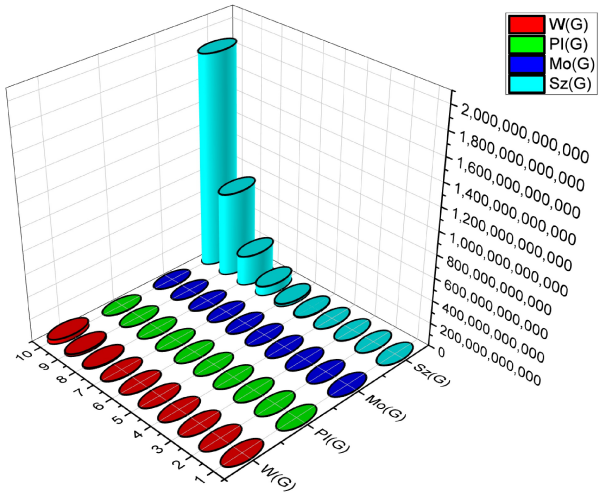

Figure 8. Comparison of graphical representation of distance-based molecular descriptors.

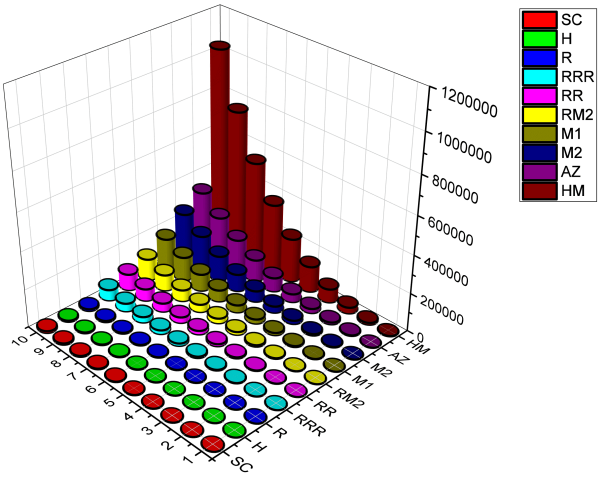

Figure 9. Comparison of graphical representation of degree-based molecular descriptors.

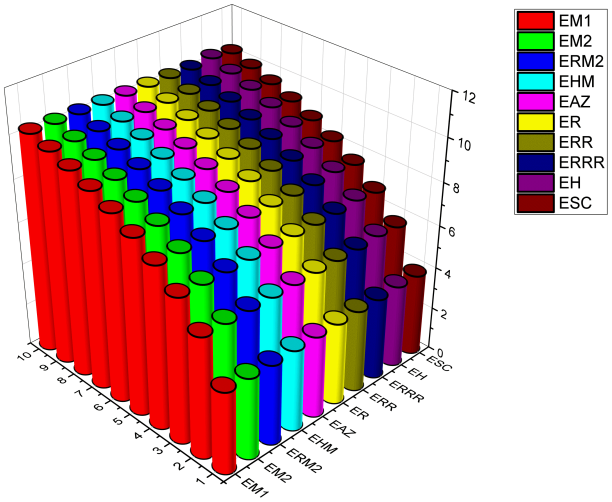

Figure 10. Comparison of entropy measures for *G*.

3.5. Statistical Correlation

All numerical values of molecular descriptors are approaches to the entropy properties of G (see Table 5). The correlation (r) gauge chart shows how strongly two quantitative variables are correlated. Pearson's correlation coefficient (r) is defined as follows.

$$r = \frac{\sum(t_i - t^-)(s_i - s^-)}{\sqrt{\sum(t_i - t^-)^2 \sum(s_i - s^-)^2}}.$$

where r = correlation coefficient,
t_i = values of the t-variable in a sample;
t^- = mean the values of the t-variable;
s_i = values of the s-variable in a sample;
s^- = mean the values of the s-variable.

We have shown the correlation (r) between degree-based descriptors (A) and degree entropy values (B) below in Table 6 and the correlation between A and B is denoted as $A \sim B$.

Table 5. Numerical values for degree-based entropies.

(n, l, k)	$(1,1,1)$	$(2,2,2)$	$(3,3,3)$	$(4,4,4)$	$(5,5,5)$	$(6,6,6)$	$(7,7,7)$	$(8,8,8)$	$(9,9,9)$	$(10,10,10)$
$EM_1(G)$	3.8625	5.6801	6.8006	7.6137	8.2525	8.7787	9.2262	9.6155	9.96	10.269
$EM_2(G)$	3.8383	5.6711	6.7961	7.6111	8.2507	8.7775	9.2253	9.6148	9.9594	10.2685
$ERM_2(G)$	3.7907	5.6552	6.7883	7.6064	8.2477	8.7753	9.2237	9.6135	9.9584	10.2677
$EHM(G)$	3.8404	5.6719	6.7965	7.6113	8.2509	8.7776	9.2254	9.6148	9.9595	10.2685
$EAZ(G)$	3.8576	5.678	6.7995	7.6131	8.2521	8.7784	9.226	9.6153	9.9599	10.2689
$ER(G)$	3.8599	5.6782	6.7995	7.6131	8.2521	8.7784	9.226	9.6153	9.9599	10.268
$ERR(G)$	3.862	5.6798	6.8005	7.6137	8.2525	8.7787	9.2262	9.6155	9.96	10.269
$EH(G)$	3.8928	5.7735	6.9177	7.7412	8.3854	8.9147	9.3642	9.7548	10.1002	10.4098
$ESC(G)$	3.8552	5.6756	6.7976	7.6113	8.2504	8.7769	9.2245	9.6138	9.9584	10.2674

Table 6. Statistical Correlation (r) between degree-based molecular descriptors and degree-based entropy values.

(n, l, k)	$M_1 \sim EM_1$	$M_2 \sim EM_2$	$RM_2 \sim ERM_2$	$HM \sim EHM$	$AZ \sim EAZ$
r	0.800895321	0.799930694	0.798222338	0.800014703	0.800664403
(n, l, k)	$R \sim ER$	$RR \sim ERR$	$RRR \sim ERRR$	$H \sim EH$	$SC \sim ESC$
r	0.822763752	0.80086312	0.800240768	0.798861487	0.801363561

The results show that vertex-based indices of this study have perfect linear relationships. As a result, all the indices mentioned in this study are extremely useful in determining the topological properties of $mSHL(n,l,k)$. As a result, the Randić index has a perfect linear relationship index for $mSHL(n,l,k)$. The effect of this paper, based on applications and properties, is beneficial in obtaining the scientific results of aluminophosphate structure for future studies.

4. Conclusions

This study computed synthetic structural descriptors for aluminophosphate-based molecular sieve structure $mSHL(n,l,k)$ using cut methods for vertex and edge-weighted molecular graphs. Entropy calculations for degree-based descriptors and linear correlation calculations for $mSHL(n,l,k)$ were carried out. Topological methods can also obtain quantitative data for phase transitions and other material alterations caused by chemical interactions, contaminants and heavy metal ions. The graphical presentation of this work, the linear correlation and the numerical comparison of the computed results will be helpful to theoretical chemists. This computational study is extremely useful in determining specific applications, such as the topological properties of the aluminophosphate structure. Further analyzing this study, we hope our results will support researchers in predicting the

NMR pattern for NMR signal processing. Moreover, it helps investigators to obtain new ideas in hypothetical and investigational NMR Spectroscopy [63–65].

Author Contributions: J.S.V.: Data collection, Writing of an original draft preparation, Visualization, Software, Methodology and Investigation. S.R.: Conceptualization, Supervision, Investigation, Reviewing and Editing. B.C.B.: Visualization, Investigation, Reviewing and Editing. M.N.H.: Visualization, Investigation. T.A.: Writing of an original draft preparation, Software. R.U.G.: Conceptualization, Investigation. M.E.: Visualization, Investigation. All authors have read and agreed to the published version of the manuscript.

Funding: We thank Universiti Malaysia Terengganu for providing funding support for this project (UMT/TAPE-RG/2021/55330).

Data Availability Statement: No data associated in the manuscript.

Acknowledgments: We thank Universiti Malaysia Terengganu for providing funding support for this project (UMT/TAPE-RG/2021/55330).

Conflicts of Interest: The authors declare no competing interests.

References

1. Wang, Y.; Zou, X.; Sun, L.; Rong, H.; Zhu, G. A zeolite-like aluminophosphate membrane with molecular-sieving property for water desalination. *Chem. Sci.* **2018**, *9*, 2533–2539. [CrossRef]
2. Yang, M.; Fan, D.; Wei, Y.; Tian, P.; Liu, Z. Recent progress in methanol-to-olefins (MTO) catalysts. *Adv. Mater.* **2019**, *31*, 1902181. [CrossRef]
3. Huang, Z.; Seo, S.; Shin, J.; Wang, B.; Bell, R.G.; Hong, S.B.; Zou, X. 3D-3D topotactic transformation in aluminophosphate molecular sieves and its implication in new zeolite structure generation. *Nat. Commun.* **2020**, *11*, 3762. [CrossRef]
4. Yu, J.; Xu, R. Insight into the construction of open-framework aluminophosphates. *Chem. Soc. Rev.* **2006**, *35*, 593–604. [CrossRef]
5. Cheetham, A.K.; Férey, G.; Loiseau, T. Open-framework inorganic materials. *Angew. Chem. Int. Ed.* **1999**, *38*, 3268–3292.
6. Liu, Z.; Xu, J.; Xu, M.; Huang, C.; Wang, R.; Li, T.; Huai, X. Ultralow-temperature-driven water-based sorption refrigeration enabled by low-cost zeolite-like porous aluminophosphate. *Nat. Commun.* **2022**, *13*, 193. [CrossRef]
7. Gozalbes, R.; Doucet, J.P.; Derouin, F. Application of topological descriptors in QSAR and drug design: History and new trends. *Curr. Drug Targets-Infect. Disord.* **2002**, *2*, 93–102. [CrossRef]
8. Arockiaraj, M.; Clement, J.; Tratnik, N.; Mushtaq, S.; Balasubramanian, K. Weighted Mostar indices as measures of molecular peripheral shapes with applications to graphene, graphyne and graphdiyne nanoribbons. *SAR QSAR Environ. Res.* **2020**, *31*, 187–208. [CrossRef]
9. Gutman, I. A formula for the Wiener number of trees and its extension to graphs containing cycles. *Graph Theory Notes NY* **1994**, *27*, 9–15.
10. Gutman, I.; Ashrafi, A.R. The edge version of the Szeged index. *Croat. Chem. Acta* **2008**, *81*, 263–266.
11. Khadikar, P.V.; Karmarkar, S.; Agrawal, V.K. A novel PI index and its applications to QSPR/QSAR studies. *J. Chem. Inf. Comput. Sci.* **2001**, *41*, 934–949. [CrossRef] [PubMed]
12. Khalifeh, M.H.; Yousefi-Azari, H.; Ashrafi, A.R.; Gutman, I. The edge Szeged index of product graphs. *Croat. Chem. Acta* **2008**, *81*, 277–281.
13. Khalifeh, M.H.; Yousefi-Azari, H.; Ashrafi, A.R.; Wagner, S.G. Some new results on distance-based graph invariants. *Eur. J. Comb.* **2009**, *30*, 1149–1163. [CrossRef]
14. Klein, D.J.; Lukovits, I.; Gutman, I. On the definition of the hyper-Wiener index for cycle-containing structures. *J. Chem. Inf. Comput. Sci.* **1995**, *35*, 50–52. [CrossRef]
15. Schultz, H.P. Topological organic chemistry. 1. Graph theory and topological indices of alkanes. *J. Chem. Inf. Comput. Sci.* **1989**, *29*, 227–228. [CrossRef]
16. Wiener, H. Structural determination of paraffin boiling points. *J. Am. Chem. Soc.* **1947**, 69, 17–20. [CrossRef]
17. Husin, M.N.; Ariffin, A. On the edge version of topological indices for certain networks. *Ital. J. Pure Appl. Math.* **2022**, *47*, 550–564.
18. Liu, Y.; Rezaei, M.; Farahani, M.R.; Husin, M.N.; Imran, M. The Omega polynomial and the Cluj-Ilmenau index of an infinite class of the Titania Nanotubes Tio2 (m, n). *J. Comput. Theor. Nanosci.* **2017**, *14*, 3429–3432. [CrossRef]
19. Husin, M.N.; Zafar, S.; Gobithaasan, R.U. Investigation of Atom-Bond Connectivity Indices of Line Graphs Using Subdivision Approach. *Math. Probl. Eng.* **2022**, *2022*, 6219155. [CrossRef]
20. Modabish, A.; Husin, M.N.; Alameri, A.Q.; Ahmed, H.; Alaeiyan, M.; Farahani, M.R.; Cancan, M. Enumeration of spanning trees in a chain of diphenylene graphs. *J. Discret. Math. Sci. Cryptogr.* **2022**, *25*, 241–251. [CrossRef]
21. Asif, F.; Zahid, Z.; Husin, M.N.; Cancan, M.; Taş, Z.; Alaeiyan, M.; Farahani, M.R. On Sombor indices of line graph of silicate carbide $Si_2\ C_3$ - $I[p,q]$. *J. Discret. Math. Sci. Cryptogr.* **2022**, *25*, 301–310. [CrossRef]
22. Ghani, M.U.; Campena FJ, H.; Pattabiraman, K.; Ismail, R.; Karamti, H.; Husin, M.N. Valency-Based Indices for Some Succinct Drugs by Using M-Polynomial. *Symmetry* **2023**, *15*, 603. [CrossRef]

23. Gutman, I.; Trinajstić, N. Graph theory and molecular orbitals. Total π-electron energy of alternant hydrocarbons. *Chem. Phys. Lett.* **1972**, *17*, 535–538. [CrossRef]
24. Estrada, E.; Torres, L.; Rodriguez, L.; Gutman, I. An atom-bond connectivity index: Modelling the enthalpy of formation of alkanes. *Indian J. Chem.* **1998**, *37A*, 849–855.
25. Randić, M. Characterization of molecular branching. *J. Am. Chem. Soc.* **1975**, *97*, 6609–6615. [CrossRef]
26. Zhou, B.; Trinajstić, N. On a novel connectivity index. *J. Math. Chem.* **2009**, *46*, 1252–1270. [CrossRef]
27. Vukičević; D; Furtula, B. Topological index based on the ratios of geometrical and arithmetical means of end-vertex degrees of edges. *J. Math. Chem.* **2009**, *46*, 1369–1376. [CrossRef]
28. Albertson, M.O. The irregularity of a graph. *Ars Comb.* **1997**, *46*, 219–225.
29. Gutman, I.; Togan, M.; Yurttas, A.; Cevik, A.S.; Cangul, I.N. Inverse problem for sigma index. *MATCH Commun. Math. Comput. Chem.* **2018**, *79*, 491e508.
30. Furtula, B.; Gutman, I. A forgotten topological index. *J. Math. Chem.* **2015**, *53*, 1184–1190. [CrossRef]
31. Vasilyev, A. Upper and lower bounds of symmetric division deg index. *Iran. J. Math. Chem.* **2014**, *5*, 91–98.
32. Hayat, S.; Imran, M.; Liu, J.B. An efficient computational technique for degree and distance based topological descriptors with applications. *IEEE Access* **2019**, *7*, 32276–32296. [CrossRef]
33. Hayat, S.; Ahmad, S.; Umair, H.M.; Wang, S. Distance property of chemical graphs. *Hacet. J. Math. Stat.* **2018**, *47*, 1071–1093. [CrossRef]
34. Hayat, S. Computing distance-based topological descriptors of complex chemical networks: New theoretical techniques. *Chem. Phys. Lett.* **2017**, *688*, 51–58. [CrossRef]
35. Shirdel, G.H.; Rezapour, H.; Sayadi, A.M. The hyper-Zagreb index of graph operations. *Iran. J. Math. Chem.* **2013**, *4*, 213–220.
36. Shannon, C.E. A mathematical theory of communication. *Bell Syst. Tech. J.* **1948**, *27*, 379–423. [CrossRef]
37. Rashevsky, N. Life, information theory and topology. *Bull. Math. Biophys.* **1955**, *17*, 229–235. [CrossRef]
38. Dehmer, M.; Grabner, M. The discrimination power of molecular identification numbers revisited. *MATCH Commun. Math. Comput. Chem.* **2013**, *69*, 785–794.
39. Ulanowicz, R.E. Quantitative methods for ecological network analysis. *Comput. Biol. Chem.* **2004**, *28*, 321–339. [CrossRef]
40. Imran, M.; Hayat, S. On counting polynomials of certain polyomino chains. *Bulg. Chem. Commun.* **2016**, *48*, 332–337.
41. Imran, M.; Hayat, S.; Shafiq, M.K. Computing omega and Sadhana polynomials of carbon nanotubes. *Optoelectron. Adv. Mater. Rapid Commun.* **2014**, *8*, 1218–1224.
42. Hayat, S.; Khan, S.; Khan, A.; Imran, M. Distance-based topological descriptors for measuring the π-electronic energy of benzenoid hydrocarbons with applications to carbon nanotubes. *Math. Methods Appl. Sci.* 2020, *early View*. [CrossRef]
43. Morowitz, H.J. Some order-disorder considerations in living systems. *Bull. Math. Biophys.* **1955**, *17*, 81–86. [CrossRef]
44. Manzoor, S.; Siddiqui, M.K.; Ahmad, S. On entropy measures of molecular graphs using topological indices. *Arab. J. Chem.* **2020**, *13*, 6285–6298. [CrossRef]
45. Došlić, T.; Martinjak, I.; Škrekovski, R.; Tipurić Spužević, S.; Zubac, I. Mostar index. *J. Math. Chem.* **2018**, *56*, 2995–3013. [CrossRef]
46. Djoković, D.Ž. Distance-preserving subgraphs of hypercubes. *J. Comb. Theory Ser. B* **1973**, *14*, 263–267. [CrossRef]
47. Winkler, P.M. Isometric embedding in products of complete graphs. Discret. *Appl. Math.* **1984**, *7*, 221–225.
48. Nadjafi-Arani, M.J.; Klavzar, S. Cut method and Djoković–Winkler's relation. *Electron. Notes Discret. Math.* **2014**, *45*, 153–157. [CrossRef]
49. Arockiaraj, M.; Clement, J.; Paul, D.; Balasubramanian, K. Relativistic distance-based topological descriptors of Linde type A zeolites and their doped structures with very heavy elements. *Mol. Phys.* **2021**, *119*, e1798529. [CrossRef]
50. Kavitha SR, J.; Abraham, J.; Arockiaraj, M.; Jency, J.; Balasubramanian, K. Topological characterization and graph entropies of tessellations of kekulene structures: Existence of isentropic structures and applications to thermochemistry, nuclear magnetic resonance and electron spin resonance. *J. Phys. Chem. A* **2021**, *125*, 8140–8158. [CrossRef]
51. Martínez-Franco, R.; Moliner, M.; Yun, Y.; Sun, J.; Wan, W.; Zou, X.; Corma, A. Synthesis of an extra-large molecular sieve using proton sponges as organic structure-directing agents. *Proc. Natl. Acad. Sci. USA* **2013**, *110*, 3749–3754. [CrossRef] [PubMed]
52. Balasubramanian, K. Combinatorics, big data, neural network & AI for medicinal chemistry & drug administration. *Lett. Drug Des. Discov.* **2021**, *18*, 943–948.
53. Sabirov, D.S.; Shepelevich, I.S. Information entropy in chemistry: An overview. *Entropy* **2021**, *23*, 1240. [CrossRef] [PubMed]
54. Chaudhry, F.; Shoukat, I.; Afzal, D.; Park, C.; Cancan, M.; Farahani, M.R. M-polynomials and degree-based topological indices of the molecule copper (i) oxide. *J. Chem.* **2021**, *2021*, 6679819. [CrossRef]
55. Mowshowitz, A.; Dehmer, M. Entropy and the complexity of graphs revisited. *Entropy* **2012**, *14*, 559–570. [CrossRef]
56. Arockiaraj, M.; Paul, D.; Klavžar, S.; Clement, J.; Tigga, S.; Balasubramanian, K. Relativistic distance based and bond additive topological descriptors of zeolite RHO materials. *J. Mol. Struct.* **2022**, *1250*, 131798. [CrossRef]
57. Gutman, I. Degree-based topological indices. *Croat. Chem. Acta* **2013**, *86*, 351–361. [CrossRef]
58. Arockiaraj, M.; Clement, J.; Tratnik, N. Mostar indices of carbon nanostructures and circumscribed donut benzenoid systems. *Int. J. Quantum Chem.* **2019**, *119*, e26043. [CrossRef]
59. Augustine, T.; Roy, S. Topological Study on Triazine-Based Covalent-Organic Frameworks. *Symmetry* **2022**, *14*, 1590. [CrossRef]
60. Sahaya Vijay, J.; Roy, S. Computation of Wiener Descriptor for Melamine Cyanuric Acid Structure. *Polycycl. Aromat. Compd.* **2023**, 1–15. [CrossRef]

61. Rahul, M.P.; Clement, J.; Junias, J.S.; Arockiaraj, M.; Balasubramanian, K. Degree-based entropies of graphene, graphyne and graphdiyne using Shannon's approach. *J. Mol. Struct.* **2022**, *1260*, 132797. [CrossRef]
62. Hussain, Z.; Ijaz, N.; Tahir, W.; Butt, M.T.; Talib, S. Calculating Degree Based Multiplicative Topological indices of Alcohol. *Asian J. Appl. Sci. Technol.* **2018**, *2*, 132–139. [CrossRef]
63. Balasubramanian, K. Operator algebraic methods for NMR spectroscopy, I. Generation of NMR spin species. *J. Chem. Phys.* **1983**, *78*, 6358–6368. [CrossRef]
64. Balasubramanian, K. Topological and group theoretical analysis in dynamic NMR spectroscopy. *J. Phys. Chem.* **1982**, *86*, 4668–4674. [CrossRef]
65. Raza, Z.; Arockiaraj, M.; Maaran, A.; Kavitha SR, J.; Balasubramanian, K. Topological entropy characterization, NMR and ESR spectral patterns of coronene-based transition metal organic frameworks. *ACS Omega* **2023**, *8*, 13371–13383. [CrossRef] [PubMed]